Carrageenan oligosaccharides and their degrading bacteria induce intestinal inflammation in germ-free mouse

Yeshi Yin (yinyeshi@126.com)
Zhejiang Academy of Agricultural Sciences https://orcid.org/0000-0001-6866-5525
Miaomiao Li
Ocean University of China
Weizhong Gu
Zhejiang University
Benhua Zeng
Third Military Medical University
Wei Liu
Zhejiang Academy of Agriculture of Science
Liying Zhu
Zhejiang Academy of Agriculture of Sciences
Xionge Pi
Zhejiang Academy of Agriculture of Sciences
Donald A Primerano
Marshall University
Hongwei D Yu
Marshall University
Hong Wei
Third Military Medical University
Guangli Yu
Ocean University of China
Xin Wang
Zhejiang Academy of Agriculture of Sciences

Research

Keywords: carrageenans, carrageenan oligosaccharides, oligosaccharide degrading bacteria, intestinal inflammatory, germ-free mouse

Posted Date: May 8th, 2020

DOI: https://doi.org/10.21203/rs.3.rs-26790/v1

Abstract

Background: Carrageenans (CGNs) are widely used in food and pharmaceutical industries. However, the safety of CGNs is still under debate, because degraded CGNs have been reported to promote an intestinal inflammatory response in animal models. Here, we studied the relationship among CGNs, human gut microbiota, and the host inflammatory response.

Methods: TLC was selected for detecting the degradation of KCPs by human gut microbiota *in vitro* batch fermentation system. PCR-DGGE and real time PCR were used for studying bacterial community. ESI-MS was used for KCPs structure analysis. Hematoxylin-eosin staining (HE), immunohistochemistry (IHC) and RNA-seq were used to evaluated the KCPs on host inflammation response in germ-free mice.

Results: Thin-layer chromatography (TLC) data showed that CGNs with a molecular weight (Mw) higher than 100 kDa are not degraded by human fecal microbiota, but low Mw CGNs with an Mw around ~4.5 kDa (KCOs) could be degraded by seven of eight human fecal microbiota samples. KCO degrading *B. xylanisolvens* was isolated from fecal samples, and PCR-DGGE profiling with band sequencing suggested that *B. xylanisolvens* was the key KCO degrader in the human gut. Two putative κ-carrageenase genes were identified in the genome sequence of *B. xylanisolvens*. However, their function on KCO degrading was not verified *in vitro*. And the sulfate group from KCO is not removed after *in vitro* degradation by human fecal microbiota, as shown by ESI-MS analysis. The effects of KCO and KCO degrading bacteria on the inflammatory response were investigated in germ-free mice. Increased numbers of P-P38-, CD3a-, and CD79a-positive cells were found in the colon and rectum in mice fed with KCO plus KCO degrading bacteria than in mice fed with only KCO or only *B. xylanisolvens* and *E. coli*, as shown by RNA-Seq analysis, HE staining, and IHC.

Conclusion: Our data suggested that the presence of KCO degrading bacteria promote the pro-inflammatory effects of CGNs.

Background

Carrageenans (CGNs), which are mainly extracted from red algae, are one of the three major industrial algal polysaccharide classes. CGNs are water-soluble, linear, sulphated polysaccharides with β-1-3 and α-1-4 linkage of galactose residues and additional substitute residues, including xylose, glucose, methyl esters, and pyruvate groups [1]. CGNs can be divided into kappa (κ-), iota (ι-), lambda (λ), and other types, based on the different forms of sulfate bonds in CGN molecules [2]. κ-CGN is mainly composed of D-galactose-4-sulfate and 3,6-D-anhydrogalactose, with 22% sulphate content in commercial κ-CGN [1]. Because of its linear structure, κ-CGN demonstrates good gel properties and is widely used in food and pharmaceutical industries [3, 4]. Due to the lack of CGN degrading digestive enzymes in the human upper gastrointestinal tract [5], CGNs enter the human colon and are inevitable encountered by human colonic microbiota [6]. Although several marine environment-related CGN degrading bacteria have been reported [7–11], little information is known regarding CGN degrading bacteria present in the human intestine.

Despite the fact that CGNs have been widely used in food industries for decades, their safety is still a topic of discussion [1, 12, 13]. A large number of animal experiments have shown that CGNs, particularly low-molecular-weight (low-MW) CGNs, can induce and promote the inflammatory response and intestinal cancer [14–26]. Indeed, poligeenan, which is designated as a fraction of CGN with Mw < 100 kDa, has been considered to exert deleterious impacts on the host health and recognized as food contaminant [1]. On the other hand, CGN polysaccharides are widely used as food additive and classified by the Food and Drug administration (FDA) and European Food Safety Authority as generally recognized as safe (GRAS) even in the infant formula. But both authorities recommence that CGN fragments of lower MW (< 50,000) should be exclusive from the products. Up to now, the safety concern of CGN largely results from animal studies. In consideration of the daily CGN consumption of up to 7.7 g/day for people in certain areas such as in south Florida [27], safety of CGNs needs to consider the role of colonic microbiota. Therefore, the interaction of κ-CGNs with human colonic microbiota and the subsequent influence on host health has been studied in the present study. The fragments of κ-CGNs with different MWs including 450 kDa (KCP), 100 kDa (SKCO) and 4.5 kDa (KCO) were prepared, and their fermentability by human gut microbiota was investigated by *in vitro* fermentation. KCO-degrading bacteria in the human intestinal tract were subsequently isolated and identified. Germ-free mouse model was used and demonstrated that the presence of both KCO and its degrading bacteria can exacerbate the host inflammatory response.

Results

Degradation of carrageenan by human fecal microbiota

Since Mw of κ-CGN may has a pivotal role in the host health, three fragments of κ-CGN with Mw of 450 kDa (KCP), 100 kDa (SKCO) and 4.5 kDa (KCO) were prepared and their fermentabilities by human colonic microbiota were examined using *in vitro* batch fermentation systems. The degree of degradation of KCP, SKCO, and KCO was measured by TLC and the phenol–sulfuric acid method. As shown in Fig. 1 and Supplementary Figure S1, KCP and SKCO were not degraded by any of the eight fecal microbiota samples. In contrast, over 50% of input KCO was degraded by six of the eight samples (K1, K2, K5, K6, K7 and K8), as measured by the phenol–sulfuric acid method with the fermentation sample collected at 24 h and 48 h; fecal samples No. K3 and No. K4 demonstrated weak KCO degradation (29.1% and 1.4% of degradation rate at 48 h) (Fig. 1B).

Acetic, propionic, and butyric fatty acids are the main Short Chain Fatty Acids (SCFAs) produced by intestinal microbiota. The concentrations of these SCFAs were measured before and after *in vitro* fermentation using HPLC analysis. As shown in Fig. 1C, the concentrations of propionic and butyric acid were significantly increased after KCO fermentation. The pH values after KCP, SKCO, and KCO fermentation were also measured. Consistent with our TLC results that KCP and SKCO are not degraded by human gut microbiota, pH values were significantly decreased only after KCO fermentation (Fig. 1D).

Kco Were Not Desulfurized By Human Colonic Microbiota

Since KCO contain sulfate groups and were degraded during fermentation, we investigated whether KCO were desulfurized in this process. Based on TLC and total carbohydrate analysis, we analyzed the structure of fermentation products from fecal samples No. K6 and No. K8, which showed the greatest extent of degradation, by gel filtration chromatography coupled with ESI-MS. The profiles of the degradation products of samples No. K6 and No. K8 were similar. Four fragments were identified as 4-*O*-sulfate-D-galactose (G4S, Degree of polymerization (dp) = 1), κ-carrabiose (dp = 2), κ-carratriose (dp = 3), and κ-carrapentaose (dp = 5) (Table 1). Desulfation was not observed during KCO degradation by human fecal microbiota.

Table 1
Data and sequence analysis of fermentation broth of feces samples No. K6 and No. K8 by electrospray ionization mass spectrometry.

Fraction	Found ions (charge)	Calculated mol mass (Na form)	Assignment		Theoretical mol mass (Na form)
			DP	Sequences	
F1	259.02 (-1)	282.02	1	G4S, salt	282.02
F2	403.06 (-1)	426.06	2	A-G4S	426.06
F3	322.03 (-2)	690.06	3	G4S-A-G4S	690.07
F4	343.03 (-3)	1098.09	5	G4S-A-G4S-A-G4S	1098.12
G4S: D-galactose-4-sulfate; A: 3,6- D-anhydrogalactose.					

KCO fermentation influenced the composition of human fecal microbiota communities

To detect the effects of KCO on human fecal microbiota communities *in vitro*, qPCR with primer pairs for the six bacterial groups *Bacteroides– Prevotella*, *Clostridium* cluster XIVab, *Bifidobacterium*, *Lactobacillus*, Enterobacteriaceae, and *Desulfovibrio* was carried out to detect changes in the relative abundance of major groups of colonic bacteria upon KCO *in vitro* fermentation. As shown in Supplementary Table S1, the relative abundance of *Bacteroides– Prevotella*, *Bifidobacterium*, *Clostridium* cluster XIVab, *Lactobacillus*, Enterobacteriaceae, and *Desulfovibrio* was not significantly different from the control group after 48 h of fermentation. *Desulfovibrio* is an indispensable member of commensal microbes in the gut that has potent sulfate reducing activity. We did observe an increase in the relative abundance of *Desulfovibrio* in all of the fecal samples, regardless of the rate of KCO degradation (Supplementary Table S1), which suggested the rise of *Desulfovibrio* was not associated with KCO degradation. In addition, the structure analysis of degradation products also showed no significant desulfation detected (Table 1). Taken together, these evidences indicated that KCO might not be desulfurized during fermentation by human gut microbiota.

Isolation And Identification Of Kco Degrading Bacteria

Human sample No. 8 was collected at 48 h after fermentation and spread on a KCO agar plate (basic growth medium VI plus 8 g/l KCO and 12 g/l agar) using a 10-fold dilution method. Colonies obtained from the plates were randomly picked and re-inoculated into KCO containing growth medium. KCO degradation was assessed using TLC analysis of the supernatant and confirmed by gel filtration chromatography and ESI-MS. Positive colonies were further purified by repeating the 10-fold dilution method.

The isolates that demonstrated an ability to degrade KCOs were identified by sequencing their 16S rRNA gene. In brief, genomic DNA was extracted using OMEGA Bacterial Genome DNA extraction kit, and the 16S rRNA gene was amplified by PCR with primers 27F (5'-CAG AGT TTG ATC CTG GCT-3') and 1492R (5'-AGG AGG TGA TCC AGC CGC A-3') [58]. DNA sequencing was conducted by Shanghai Sangon Biotech Co., Ltd. (Shanghai, China). Bacterial species were identified using BLAST searches for aligned 16S rRNA gene sequences (http://blast.ncbi.nlm.nih.gov/Blast.cgi).

GO term	GF-GNK	GF-GN	GF-GFK
nucleotide binding	185		
calcium ion binding	92		
carbohydrate binding	56	17	
structural molecule activity	53		
pattern binding	35		
polysaccharide binding	35		
glycosaminoglycan binding	31		
protein tyrosine kinase activity	26		
heparin binding	25		
growth factor binding	21		
transmembrane receptor protein tyrosine kinase activity	13		
extracellular matrix structural constituent	12		
extracellular matrix binding	9		
platelet-derived growth factor binding	7		
vascular endothelial growth factor receptor activity	5		
glutathione transferase activity			10
transferase activity, transferring alkyl or aryl (other than methyl) groups			10

* Arabic numerals represent the numbers of DEGs classified in these GO terms.

Table 2.

GOs at the molecular functional level of DEGs.

Discussion

κ-CGNs are sulfurized seaweed polysaccharides with thermo-reversible gelling properties that are widely used as food thickening agent. However, the safety of κ-CGNs remains a concern [1]. Accumulating evidence indicates that κ-CGNs, especially their low-MW degradation products, induce inflammation in the colon, resulting in a range of diseases in cell and animal models, including thrombosis [28–31],

peritonitis [26, 32–34], paw edema [35, 36], pleurisy [37, 38], gastroenterocolitis [39, 40], arthritis [41, 42], and inflammatory bowel disease. However, CGNs also show positive health effects, such as antitumor [43], antimicrobial [44], and antiviral [45, 46]. The inconsistent effects of κ-CGN have been attributed to the varying MWs of compounds present in commercial κ-CGN products [1], but we propose that the variation in composition and function of human colonic microbiota may also contribute to the dilemma

Therefore, in the present study, we investigated the interaction of κ-CGNs of different MWs with human colonic microbiota. The results clearly demonstrate that the κ-CGN degradation rate by human gut microbiota is correlated with the MW of the κ-CGNs. κ-CGNs with an MW over 100 kDa, which include both KCP and SKCO, cannot be utilized by human fecal microbiota *in vitro* (Supplementary Figure S1), while the degradation of low MW CGNs of approximately 4.5 kDa (KCO) varied among volunteer fecal samples (Fig. 1) suggesting the KCO degradation is also dependent on the composition of the human microbiomes.

Removal of sulfate esters from sulfated polysaccharides is considered one of the essential steps for microorganisms in the degradation of sulfurized polysaccharides [47]. The most diversified sulfatase genes have been discovered in marine bacteria [48], due to the higher contents of sulfate ester groups in marine polysaccharides. The human intestinal tract contains high amounts of sulfurized glycans. For example, mucins, heparan sulfate, and chondroitin sulfate, which are the main components of the extracellular matrix of mammalian cells, can be degraded by human colonic microbiota; bacterial sulfatases have also been identified from mucin degrading bacterial strains [49, 50]. *Bacteroides thetaiotaomicron*, which has 28 putative sulfatase genes, is able to liberate free sulfate from chondroitin to provide it as the electron acceptor for the sulfate reducing bacterium *Desulfovibrio piger* in the mouse gut, releasing H_2S as the end product [51]. It is known that H_2S can act as a signaling molecule, exerting detrimental effects on colonocytes; it remains to be elucidated whether free sulfate can be released from CGNs by human colonic microbiota. Based on the structure analysis of KCO fragments after fermentation by human fecal microbiota, the major derivatives identified in the present study are 4-*O*-sulfate-D-galactose, κ-carrabiose, κ-carratriose, and κ-carrapentaose, suggesting sulfate is not hydrolyzed from KCO. The qPCR data showed that the total abundance of *Desulfovibrio* did not change under different KCO degradation rates. These data indicate that human colonic microbiota are able to degrade KCO, but do not remove sulfate from KCO or their derivatives, which is consistent with the previous observation [52]. Therefore, enzymes from human colonic microbiota for degrading marine sulfated polysaccharides may differ from the ones used for degradation of sulfurized glycans of human origin.

Whereas several strains of marine CGN degrading bacteria have been isolated [7–11], few studies have been reported on the CGN degrading bacteria in animal or human intestines. By *in vitro* KCO-based batch fermentation and degradation screening, a KCO-degrading species, *B. xylanisolvens*, and its partner strain, *E. coli*, were identified. Similar to a previous report [53], the presence of *E. coli* improved the KCO degradation ability of *B. xylanisolvens*, suggesting a cross-feeding phenomenon exists between the KCO degrader and *E. coli* [53]. We hypothesize that *E. coli* can utilize the metabolites generated by *B. xylanisolvens*, particularly galactose, thereby reducing the negative feedback of monosaccharide

degradation products (on carrageenase synthesis) in *B. xylanisolvens* and improving its KCO degradation capacity [53]. Moreover, PCR-DGGE analysis and DGGE band sequencing showed that KCO could promote the growth of *B. xylanisolvens* in five of eight fecal samples with KCO degradation capacity (Fig. 2C), confirming *B. xylanisolvens* plays a key role in the utilization of KCO by human colonic microbiota. Two genes homologous to κ-carrageenase usage were identified by bioinformatic analysis, but no KCO degradation activity is detected after transformation of the two genes into *E. coli*. The mechanism by which *B. xylanisolvens* degrades KCO remains to be further studied.

Although the impact of carageenans on colonic immune response has been investigated previously, the effects of CGN degradation products and the bacteria that degrade them on the host inflammatory response were not investigated yet. Germ-free mice were given (i) KCO, (ii) *B. xylanisolvens* and *E. coli*, (iii) KCO plus *B. xylanisolvens* and *E. coli*, or (iv) water (control). Interestingly, inflammation scores (evaluated by H&E staining) were significantly higher in colon and rectum than in duodenum, jejunum, and ileum; and the combination of KCO plus KCO degrading bacteria had a stronger pro-inflammatory effect than the other groups. As demonstrated previously, administration of CGN into the mouse pleural cavity can induce pleurisy through the activation of the P38 MAPK pathway; up-regulated p38 and p-p38 levels were observed in mouse rectum samples, in particular in mice treated with KCO plus *B. xylanisolvens* and *E. coli*. IHC with p-p38 analysis revealed a low degree of inflammation in the group treated with *B. xylanisolvens* and *E. coli* or KCO, but a significant increase in inflammation was observed in the group treated with KCO plus *B. xylanisolvens* and *E. coli*, confirming the KCO degradation products lead to tissue inflammation in the mouse rectum. Since KCO treatment alone also causes low grade inflammation compared to GF mice and significant increased inflammation is observed in the group treated by the combination KCO and KCO degradation bacteria, we infer that the enhancement of inflammation is ascribed to the derivatives of KCO generated by the presence of KCO degradation bacteria. Indeed, small Mw of CGN has greater diffusion rates through the mucus layer to affect intestinal epithelium [1]. In addition, since the degradation of KCO by colonic microbiota required at least 48 hours incubation, KCO degradation is most likely occurred at the anatomical positions of colon and rectum.

Cell-to-cell and cell-to-matrix adherence are essential for maintaining proper epithelial tissue homeostasis. KEGG analysis showed DEGs were mainly involved in leukocyte transendothelial migration. Among the DEGs, VCAM1, JAM2, JAM3, PECAM1, VCAM1, and CDH5 encode key proteins in the process of diapedesis; the mRNA levels of all six genes were decreased in mice treated with KCO plus *B. xylanisolvens* and *E. coli*, implying the metabolites generated from KCO degradation may reduce the adherence of tight junctions of epithelial and endothelial cells [54]. Differential expression of JAM2 and JAM3 is always found in tumor and adjacent tissues [55], implying that the pro-inflammatory effects of KCOs and KCO degrading bacteria may contribute to the increase in gut permeability.

Conclusions

In summary, high-MW κ-CGNs (> 100 kDa) cannot be degraded by human intestinal microflora *in vitro*, while gut microbiota from six of eight volunteers could degrade and utilize 4.5-kDa KCO *in vitro*. *B.*

xylanisolvens and *E. coli* work in synergistically to degrade KCO; however, they were unable to remove the sulfate group from KCO and their derivatives. Experiments with germ-free mice suggested that KCO, a combination of *B. xylanisolvens* and *E. coli*, and KCO plus KCO degrading bacteria can exert pro-inflammatory effects on the colon and rectum of mice. Therefore, our results suggest that, in addition to the presence of low-MW CGNs, the presence of KCO degrading bacteria is a promote factor in the pro-inflammatory effects and safety of CGNs.

Methods

Study design

To better understand the interactions of different molecular weight kappa carrageenan polysaccharides (KCPs) with human gut microbiota and host health, the degradation of KCP, SKCO and KCO by human gut microbiota were evaluated *in vitro* first, KCO-degrading bacterial was then isolated from human fecal samples, and their effects of KCO and KCO plus KCO-degrading bacterial on germ free mouse were investigated.

Preparation Of Carrageenan Polysaccharides And Oligosaccharides

KCP were obtained from Yantai Runlong Marine Biological Products Co., Ltd., China. Two types of carrageenan oligosaccharides were obtained after hydrolysis with dilute HCl (SKCO or 732 resin plus HCl (KCO). For SKCO preparation, 10 mg/ml carrageenan was adjusted to pH 1.26 with 0.1 M HCl and then heated to 37 °C for 3 hours. For KCO preparation, 30 mg/ml carrageenan was dissolved at 70 °C, and treated with 732 resin for 4 hours. The hydrolytic product was neutralized with 1 M NaOH and put into a dialysis bag (MW cutoff was 200–500 Da) to remove the salt. The final product was obtained by rotary evaporation and lyophilization. The MW of KCP, SKCO, and KCO was measured using high-performance liquid chromatography (HPLC) (Agilent 1260, U.S.) with a Shodex OH pak SB-804 HQ column, detected using a refractive index detector and multiangle laser light scattering. The average MWs of KCP, SKCO, and KCO were 450 kDa, 100 kDa, and 4.5 kDa, respectively.

Electrospray ionization mass spectrometry (ESI-MS) for sugar structure analysis

The derivatives generated from digestion of CGN oligosaccharides were determined by gel filtration chromatography and analyzed using negative-ion electrospray ionization mass spectrometry (ESI-MS). In brief, after removing the bacteria by centrifugation, the supernatants were separated on a Superdex Peptide 10/300 column. The sequence of each fraction was determined on a Thermo LTQ Orbitrap XL instrument (Thermo Finnigan Corp, U.S.). Samples were then dissolved in CH_3CN/H_2O (1:1, v/v) at a

concentration of 10 pmol/μl and 5 μl was injected. Solvent volatilization temperature and capillary temperatures were 275 °C. The sheath flow gas flow rate was 8 arb. The flow rate was 8 μl/min during ESI-MS analysis. Helium was used as collision gas, with a collision energy of 20–25 eV.

Origin Of Human Fecal Samples

Eight healthy human volunteers (from Hangzhou, China), between 24 and 27 years of age, were recruited for the current study. The donors had not received antibiotics or pro- or prebiotic treatment for at least three months prior to sample collection. All of the volunteers provided informed, written consent, and the study was approved by the Ethics Committee of the Zhejiang Academy of Agricultural Sciences.

Batch culture fermentation of KCP, SKCO, and KCO with human fecal slurries

Batch culture fermentation was conducted using the procedure described by Lei et al. [56]. Briefly, basic growth medium VI contained the following components (g/l): yeast extract, 4.5; tryptone, 3.0; peptone, 3.0; bile salts No. 3, 0.4; L-cysteine hydrochloride, 0.8; hemin, 0.05; NaCl, 4.5; KCl, 2.5; $MgCl_2.6H_2O$, 0.45; $CaCl_2.6H_2O$, 0.2; KH_2PO_4, 0.4; Tween 80, 1 ml; and 2 ml of a solution of trace elements. To assess the degradation and utilization by human fecal microbiota, either 1.0 g of KCP, 5.0 g of SKCO, and 8.0 g of KCO were added as the sole carbon source. Due to the viscosity of KCP and SKCO, the amount of KCP and SKCO in the medium was reduced compared to KCO. The media were adjusted to pH 6.5 before autoclaving. Fresh fecal samples were homogenized in stomacher bags with 0.1 M anaerobic phosphate-buffered saline (PBS) (pH 7.0) to make 10% (wt/vol) slurry. Large food residues were removed by passing the mixture through a 0.4 mm sieve. The human fecal slurry (7 ml) was inoculated into a bottle containing 63 ml of growth medium, and the bottle was incubated at 37 °C for 72 h in an anaerobic chamber (anaerobic workstation AW 500, Electrotek Ltd., U.K.). Fermentation products were collected at different time points for further analysis. The pH value after 48 h fermentation was measured by a pH probe (Eutech, Singapore).

Thin-layer Chromatography (tlc) And Total Carbohydrate Analysis

The degradation of KCP, SKCO, and KCO was detected by TLC analysis. Briefly, 0.2 μL of sample was loaded on pre-coated silica gel-60 TLC aluminum plates (Merck, Germany). After development with a solvent system consisting of formic acid/n-butanol/water (6:4:1, v:v:v), the plate was soaked in orcinol reagent and carbohydrates were visualized by heating at 120 °C for 3 min.

The total carbohydrate concentration in the fermentation samples was determined using the phenol–sulfuric acid method, as described previously, using D-galactose as standard. Results are expressed as

the mean amount of remaining carbohydrate relative to the total amount detected at 0 h.

Quantitation Of Bacterial Groups By Real-time Pcr

Quantification of bacterial DNA was performed using an ABI PRISM 7500 Real-Time PCR Detection System (Applied Biosystems) according to the manufacturer's instructions. A 20-μl amplification reaction was performed with 10 μl Thunderbird SYBR qPCR Mix (Toyobo Co., Ltd, Osaka, Japan), 0.04 μl 50 × ROX reference dye, 0.5 mM of each primer, 1 μl DNA template (20 ng/μl), and distilled water. Amplifications were performed with the following PCR program: one cycle at 95 °C for 1 min, 40 cycles at 95 °C for 15 s, an appropriate annealing temperature for 35 s, and 72 °C for 35 s. Fluorescence was measured after the extension phase of each cycle. Melt curve analyses were performed by slowly heating the PCR mixtures from 55 °C to 95 °C. These served as end point assays and were used to confirm PCR specificity. Six pairs of primers were selected for quantification of the total number of the following bacteria: *Bacteroides*–*Prevotella* group, *Bifidobacterium*, *Clostridium* cluster XI, Enterobacteriaceae, *Lactobacillus*, and *Desulfovibrio*. The primer sequences and annealing temperature for each primer pair are shown in Supplementary Table S3. The quantitative measurement of unknown samples was achieved using standard curves made with known concentrations of plasmid DNA containing the respective amplicons for each set of primers.

Short-chain Fatty Acid (scfa) Analysis

Production of short-chain fatty acids (SCFAs) was determined by HPLC with an Aminex HPX-87H Exclusion Column. In brief, fermentation products were centrifuged at 14, 000 rpm for 15 min, and the supernatant was used for measurement. The detection condition included 5 mM H_2SO_4 used as mobile phase at a flow rate of 0.6 ml/min. The column temperature was 50 °C and a refractive index detector was used at a wavelength of 215 nm.

Animal Experiments

Twenty-four three-week-old germ-free Kunming mice were randomly divided into four groups. KCO degrading bacteria (5×10^8 in 0.5 ml) were inoculated intragastrically to the GN and GNK groups on day 0. Bacterial colonization was allowed for 56 days. Fecal pellets were collected after 4 weeks from each group to check the bacterial composition and population by 16 s rRNA gene clone library sequencing. After 56 days, 5% KCO was given in drinking water in the GNK and GK groups for an additional 8 weeks. The group without any treatment (GF) was used as control. Mice were sacrificed by cervical dislocation, and serum, liver, cecal content, and gut tissue samples were collected. All the animals were handled in strict compliance with current regulations and guidelines concerning the use of laboratory animals in China. The procedures were approved by the Zhejiang Academy of Agricultural Science and Third Military Medical University.

Rna-seq Analysis

To identify genes that were differentially expressed (DEGs) in response to KCOs and KCO-degrading bacteria in germ-free mice at the transcription level, total RNA was isolated from rectum samples for RNA-Seq analysis. RNA quality was assessed by Nanodrop and electrophoresis. Samples with RNA integrity numbers ≥ 8 were prepared using the TruSeq RNA Sample Prep Kit (Illumina, San Diego, CA, USA). Multiplex amplification was used to prepare cDNA with a paired-end read length of 100 bases using an Illumina HiSeq 2000 (Illumina, Inc., San Diego, CA, USA). RNA-Seq was performed by Shanghai Personal Biotechnology Co., Ltd. (http://www.personalbio.cn/en/).

Quality control assessment of RNA-Seq data was completed using the FastQC tool (http://www.bioinformatics.babraham.ac.uk/projects/fastqc/) for high-throughput sequencing before and after RNA-Seq alignment. RNA-Seq data were analyzed using the DNABOX suite (http://www.dnabox.cn/) of sequence analysis programs, including Bowtie, TopHat, and Cufflinks. Using TopHat, the resulting FASTQ files were aligned to the NCBI reference mouse genome (Mus_musculus.GRCm38.75) to identify known transcripts. Mapped reads were processed using the Cufflinks algorithm to calculate fragments per kilobase of exon per million mapped reads (FPKM), which accurately reflects the RNA transcript number normalized for RNA length and total number of mapped reads. DEGs with a P-value < 0.05 were identified and subjected to GO and KEGG analysis using the online tool DAVID (https://david.ncifcrf.gov/).

He Staining

The duodenum, jejunum, ileum, colon, and rectum samples were immediately removed, immersed in 4% paraformaldehyde in 0.1 M PBS (pH 7.4) for 24 hours, dehydrated with dH_2O for 30 minutes, rinsed in 75% ethanol for 1 hour, 95% ethanol for 1 hour twice, 100% ethanol for 1 hour twice, and 100% xylene for 20 minutes twice, and then immersed in paraffin at 58–60 °C for 3 hours. After the tissue was paraffin-embedded, 4-μm coronal serial sections were cut using a Microm HM-340E microtome (Microm, Walldorf, Germany). The sections were subjected to HE staining and mounted with neutral balsam. Subsequently, they were examined by microscopy to observe the changes in ulcer size and infiltration of inflammatory cells. Injuries to colon tissue were scored as previously described.

Immunohistochemical (ihc) Analysis

The specimens were stained with the EnVision™ two-step strategy and high-temperature antigen retrieval (pressure cooker, Supor Co, China). In brief, 4-μm-thick paraffin-embedded sections were deparaffinized twice (10 minutes each in 100% xylene) and then hydrated with 100% ethanol for 5 minutes twice, with 95% ethanol for 3 minutes, and with 80% ethanol for 5 minutes. After two 5-minute soakings in distilled water, the slides were put into the pressure cooker filled with 1000 ml of boiling sodium citrate buffer (pH 9.0) and heated under pressure. After steaming, the pressure cooker was removed from the heat source

and cooled down to room temperature with tap water. The slides were then rinsed twice for 3 minutes with PBS. The slides were incubated with 3% hydrogen peroxide for 10 minutes and rinsed twice in PBS for 3 minutes. Primary antibody (anti-CD3, 1:100, clone SP7, ab16669, Abcam; anti-VCAM1, 1:200, clone EPR5047, ab134047, Abcam; anti-PECAM1, 1:1000, clone EPR17259, ab182981, Abcam; anti-phospho-p38 MAPK (Thr180 and Tyr182), 1:400, clones D3F9 and 4511, Cell Signaling Technology) were applied for 60 minutes in a moist chamber at 37 °C. After rinsing twice for 3 minutes with PBS, the slides were incubated with HRP polymer for 30 minutes at 37 °C. After adding diaminobenzidine (DAB) chromagen, the slides were observed and examined for color change under a light microscope. This was followed by counterstaining with hematoxylin for 1 minute and rinsing with tap water for 1 minute. Two slides were treated with PBS instead of primary antibody and served as the negative control. Sections were observed using the double-blind method by a pathological physician. In each section, cells were selected in five randomly selected fields to calculate the percentage of positive cells.

Statistical analysis

All values are presented as mean ± SEM. Statistical analyses were performed in SPSS v18.0 (SPSS Inc., Chicago, IL, United States). Data on SCFA and total carbohydrate concentrations were analyzed using two-way analysis of variance (ANOVA) and the Tukey multiple comparison tests with the Data Processing System (DPS) v16.5 [59]. Metabolites with variable importance in the projection (VIP) values > 1.0 were considered changed. Metabolomics were analyzed with a Student's *t*-test.

Declarations

Ethics approval and consent to participate

See ethics paragraph in the "Materials and methods" section.

Consent for publication

Not applicable

Availability of data and materials

Raw sequence data are accessible in NCBI database for mouse RNA-seq (PRJNA589115) and KCO-degrading bacteria draft genome (PRJNA588896).

Competing interests

The authors declare that there are no competing interests.

Funding

Xin Wang was supported by National Natural Science Foundation of China (NFSC, 2019R17A32B01) and Key Research & Development plan of Zhejiang Province (2018R17B88D03). Yeshi Yin was supported by Distinguished Young Scholars of Hunan Natural Science Foundation. HDY was supported by the National

Institutes of Health (NIH) grants R44GM113545 and P20GM103434. DAP is supported by NIGMS INBRE grant GM103434.

Authors' contributions

Conceived and designed the experiments: Xin Wang, Guangli Yu, Hong Wei, and Hongwei Yu; Performed experiments: Yeshi Yin, MiaoMiao Li, Weizhong Gu, Benhua Zeng, Wei Liu, Liying Zhu and Xionge Pi; Data analysis: Donald A Primerano, Hongwei Yu and Weizhong Gu; Wrote the paper: Yeshi Yin, MiaoMiao Li and Xin Wang.

References

1. David S, Shani Levi C, Fahoum L, Ungar Y, Meyron-Holtz EG, Shpigelman A, Lesmes U: Revisiting the carrageenan controversy: do we really understand the digestive fate and safety of carrageenan in our foods? *Food Funct* 2018, 9(3):1344-1352.
2. Campo VLK, D. F.; Silva, D. B. da; Carvalho, I.: Carrageenans: biological properties, chemical modifications and structural analysis - a review. *Carbohydr Polym* 2009, 77(2):167-180.
3. Prajapati VD, Maheriya PM, Jani GK, Solanki HK: Carrageenan: a natural seaweed polysaccharide and its applications. *Carbohydr Polym* 2014, 105:97-112.
4. Li L, Ni R, Shao Y, Mao S: Carrageenan and its applications in drug delivery. *Carbohydr Polym* 2014, 103:1-11.
5. Harmuth-Hoene AE, Schwerdtfeger E: Effect of indigestible polysaccharides on protein digestibility and nitrogen retention in growing rats. *Nutr Metab* 1979, 23(5):399-407.
6. Hehemann JH, Correc G, Barbeyron T, Helbert W, Czjzek M, Michel G: Transfer of carbohydrate-active enzymes from marine bacteria to Japanese gut microbiota. *Nature* 2010, 464(7290):908-912.
7. Jung J, Bae SS, Chung D, Baek K: Tamlana carrageenivorans sp. nov., a carrageenan-degrading bacterium isolated from seawater. *Int J Syst Evol Microbiol* 2019.
8. Shen J, Chang Y, Chen F, Dong S: Expression and characterization of a kappa-carrageenase from marine bacterium Wenyingzhuangia aestuarii OF219: A biotechnological tool for the depolymerization of kappa-carrageenan. *Int J Biol Macromol* 2018, 112:93-100.
9. Shen J, Chang Y, Dong S, Chen F: Cloning, expression and characterization of a iota-carrageenase from marine bacterium Wenyingzhuangia fucanilytica: A biocatalyst for producing iota-carrageenan oligosaccharides. *J Biotechnol* 2017, 259:103-109.
10. Park S, Won SM, Yoon JH: Dokdonia ponticola sp. nov., A Carrageenan-Degrading Bacterium of the Family Flavobacteriaceae Isolated from Seawater. *Curr Microbiol* 2018, 75(9):1126-1132.
11. Ficko-Blean E, Prechoux A, Thomas F, Rochat T, Larocque R, Zhu Y, Stam M, Genicot S, Jam M, Calteau A *et al*: Carrageenan catabolism is encoded by a complex regulon in marine heterotrophic bacteria. *Nat Commun* 2017, 8(1):1685.

12. David S, Fahoum L, Rozen G, Shaoul R, Shpigelman A, Meyron-Holtz EG, Lesmes U: Reply to the Comment on "Revisiting the carrageenan controversy: do we really understand the digestive fate and safety of carrageenan in our foods?" by M. Weiner and J. McKim, Food Funct., 2019, 10: DOI: 10.1039/C8FO01282B. *Food Funct* 2019, 10(3):1763-1766.
13. Weiner ML, McKim JM: Comment on "Revisiting the carrageenan controversy: do we really understand the digestive fate and safety of carrageenan in our foods?" by S. David, C. S. Levi, L. Fahoum, Y. Ungar, E. G. Meyron-Holtz, A. Shpigelman and U. Lesmes, Food Funct., 2018, 9, 1344-1352. *Food Funct* 2019, 10(3):1760-1762.
14. Al-Majed AA, Khattab M, Raza M, Al-Shabanah OA, Mostafa AM: Potentiation of diclofenac-induced anti-inflammatory response by aminoguanidine in carrageenan-induced acute inflammation in rats: the role of nitric oxide. *Inflamm Res* 2003, 52(9):378-382.
15. Beloeil H, Asehnoune K, Moine P, Benhamou D, Mazoit JX: Bupivacaine's action on the carrageenan-induced inflammatory response in mice: cytokine production by leukocytes after ex-vivo stimulation. *Anesth Analg* 2005, 100(4):1081-1086.
16. da Rosa JS, de Mello SV, Vicente G, Moon YJ, Daltoe FP, Lima TC, de Jesus Souza R, Biavatti MW, Frode TS: Calea uniflora Less. attenuates the inflammatory response to carrageenan-induced pleurisy in mice. *Int Immunopharmacol* 2017, 42:139-149.
17. Dos Reis GO, Vicente G, de Carvalho FK, Heller M, Micke GA, Pizzolatti MG, Frode TS: Croton antisyphiliticus Mart. attenuates the inflammatory response to carrageenan-induced pleurisy in mice. *Inflammopharmacology* 2014, 22(2):115-126.
18. Houshmand G, Mansouri MT, Naghizadeh B, Hemmati AA, Hashemitabar M: Potentiation of indomethacin-induced anti-inflammatory response by pioglitazone in carrageenan-induced acute inflammation in rats: Role of PPARgamma receptors. *Int Immunopharmacol* 2016, 38:434-442.
19. Ito NM, Noronha AM, Bohm GM: Carrageenan-induced acute inflammatory response in chicks. *Res Vet Sci* 1989, 46(2):192-195.
20. Joe B, Garrett MR, Dene H, Remmers EF, Meng H: Genetic susceptibility to carrageenan-induced innate inflammatory response in inbred strains of rats. *Eur J Immunogenet* 2003, 30(4):243-247.
21. Moilanen LJ, Laavola M, Kukkonen M, Korhonen R, Leppanen T, Hogestatt ED, Zygmunt PM, Nieminen RM, Moilanen E: TRPA1 contributes to the acute inflammatory response and mediates carrageenan-induced paw edema in the mouse. *Sci Rep* 2012, 2:380.
22. Myers MJ, Deaver CM, Lewandowski AJ: Molecular mechanism of action responsible for carrageenan-induced inflammatory response. *Mol Immunol* 2019, 109:38-42.
23. Nader M, Vicente G, da Rosa JS, Lima TC, Barbosa AM, Santos AD, Barison A, Dalmarco EM, Biavatti MW, Frode TS: Jungia sellowii suppresses the carrageenan-induced inflammatory response in the mouse model of pleurisy. *Inflammopharmacology* 2014, 22(6):351-365.
24. Pham-Marcou TA, Gentili M, Asehnoune K, Fletcher D, Mazoit JX: Effect of neurolytic nerve block on systemic carrageenan-induced inflammatory response in mice. *Br J Anaesth* 2005, 95(2):243-246.

25. Schrier DJ, Lesch ME, Wright CD, Gilbertsen RB: The antiinflammatory effects of adenosine receptor agonists on the carrageenan-induced pleural inflammatory response in rats. *J Immunol* 1990, 145(6):1874-1879.
26. Syam S, Bustamam A, Abdullah R, Sukari MA, Hashim NM, Mohan S, Looi CY, Wong WF, Yahayu MA, Abdelwahab SI: beta Mangostin suppress LPS-induced inflammatory response in RAW 264.7 macrophages in vitro and carrageenan-induced peritonitis in vivo. *J Ethnopharmacol* 2014, 153(2):435-445.
27. Shah Z C HFG: Current availability and consumption of carrageenan-containing foods. *Ecology of Food and Nutrition* 2003, 42(6):357-371.
28. Arslan R, Bor Z, Bektas N, Mericli AH, Ozturk Y: Antithrombotic effects of ethanol extract of Crataegus orientalis in the carrageenan-induced mice tail thrombosis model. *Thromb Res* 2011, 127(3):210-213.
29. Li Q, Chen Y, Zhao D, Wei Z, Zhang S, Chen Y, Wang Y, Qian K, Zhao B, Zhu Y *et al*: NaoXinTong Capsule Inhibits Carrageenan-Induced Thrombosis in Mice. *J Cardiovasc Pharmacol* 2018, 72(1):49-59.
30. Simkhada JR, Cho SS, Mander P, Choi YH, Yoo JC: Purification, biochemical properties and antithrombotic effect of a novel Streptomyces enzyme on carrageenan-induced mice tail thrombosis model. *Thromb Res* 2012, 129(2):176-182.
31. Yan F, Yan J, Sun W, Yao L, Wang J, Qi Y, Xu H: Thrombolytic effect of subtilisin QK on carrageenan induced thrombosis model in mice. *J Thromb Thrombolysis* 2009, 28(4):444-448.
32. Alves CF, Alves VB, de Assis IP, Clemente-Napimoga JT, Uber-Bucek E, Dal-Secco D, Cunha FQ, Rehder VL, Napimoga MH: Anti-inflammatory activity and possible mechanism of extract from Mikania laevigata in carrageenan-induced peritonitis. *J Pharm Pharmacol* 2009, 61(8):1097-1104.
33. Barth CR, Funchal GA, Luft C, de Oliveira JR, Porto BN, Donadio MV: Carrageenan-induced inflammation promotes ROS generation and neutrophil extracellular trap formation in a mouse model of peritonitis. *Eur J Immunol* 2016, 46(4):964-970.
34. de Souza Costa M, Teles RHG, Dutra YM, Neto J, de Brito TV, de Sousa Nunes Queiroz FF, do Vale DBN, de Souza LKM, Silva IS, Dos Reis Barbosa AL *et al*: Photobiomodulation reduces neutrophil migration and oxidative stress in mice with carrageenan-induced peritonitis. *Lasers Med Sci* 2018, 33(9):1983-1990.
35. Labrecque G, Belanger PM, Dore F: Circannual variations in carrageenan-induced paw edema and in the anti-inflammatory effect of phenylbutazone in the rat. *Pharmacology* 1982, 24(3):169-174.
36. Moon SM, Lee SA, Hong JH, Kim JS, Kim DK, Kim CS: Oleamide suppresses inflammatory responses in LPS-induced RAW264.7 murine macrophages and alleviates paw edema in a carrageenan-induced inflammatory rat model. *Int Immunopharmacol* 2018, 56:179-185.
37. Bayir Y, Un H, Cadirci E, Akpinar E, Diyarbakir B, Calik I, Halici Z: Effects of Aliskiren, an RAAS inhibitor, on a carrageenan-induced pleurisy model of rats. *An Acad Bras Cienc* 2019, 91(1):e20180106.
38. Capasso F, Dunn CJ, Yamamoto S, Willoughby DA, Giroud JP: Further studies on carrageenan-induced pleurisy in rats. *J Pathol* 1975, 116(2):117-124.

39. Tkachenko A, Marakushyn D, Kalashnyk I, Korniyenko Y, Onishchenko A, Gorbach T, Nakonechna O, Posokhov Y, Tsygankov A: A study of enterocyte membranes during activation of apoptotic processes in chronic carrageenan-induced gastroenterocolitis. *Med Glas (Zenica)* 2018, 15(2):87-92.
40. Martino JV, Van Limbergen J, Cahill LE: The Role of Carrageenan and Carboxymethylcellulose in the Development of Intestinal Inflammation. *Front Pediatr* 2017, 5:96.
41. Herlin T, Fogh K, Ewald H, Hansen ES, Knudsen VE, Holm I, Kragballe K, Bunger C: Changes in lipoxygenase products from synovial fluid in carrageenan induced arthritis in dogs. *APMIS* 1988, 96(7):601-604.
42. Jitta SR, Daram P, Gourishetti K, Misra CS, Polu PR, Shah A, Shreedhara CS, Nampoothiri M, Lobo R: Terminalia tomentosa Bark Ameliorates Inflammation and Arthritis in Carrageenan Induced Inflammatory Model and Freund's Adjuvant-Induced Arthritis Model in Rats. *J Toxicol* 2019, 2019:7898914.
43. Luo M, Shao B, Nie W, Wei XW, Li YL, Wang BL, He ZY, Liang X, Ye TH, Wei YQ: Antitumor and Adjuvant Activity of lambda-carrageenan by Stimulating Immune Response in Cancer Immunotherapy. *Sci Rep* 2015, 5:11062.
44. Inic-Kanada A, Stein E, Stojanovic M, Schuerer N, Ghasemian E, Filipovic A, Marinkovic E, Kosanovic D, Barisani-Asenbauer T: Effects of iota-carrageenan on ocular Chlamydia trachomatis infection in vitro and in vivo. *J Appl Phycol* 2018, 30(4):2601-2610.
45. Grassauer A, Weinmuellner R, Meier C, Pretsch A, Prieschl-Grassauer E, Unger H: Iota-Carrageenan is a potent inhibitor of rhinovirus infection. *Virol J* 2008, 5:107.
46. Guo C, Zhu Z, Yu P, Zhang X, Dong W, Wang X, Chen Y, Liu X: Inhibitory effect of iota-carrageenan on porcine reproductive and respiratory syndrome virus in vitro. *Antivir Ther* 2019.
47. Barbeyron T, Brillet-Gueguen L, Carre W, Carriere C, Caron C, Czjzek M, Hoebeke M, Michel G: Matching the Diversity of Sulfated Biomolecules: Creation of a Classification Database for Sulfatases Reflecting Their Substrate Specificity. *PLoS One* 2016, 11(10):e0164846.
48. Helbert W: Marine Polysaccharide Sulfatases. *Front Mar Sci* 2017, 4(6): doi: 10.3389/fmars.2017.00006.
49. Van Eldere J, Robben J, De Pauw G, Merckx R, Eyssen H: Isolation and identification of intestinal steroid-desulfating bacteria from rats and humans. *Appl Environ Microbiol* 1988, 54(8):2112-2117.
50. Gibson GRC, J.H. Macfarlane, G.T.: Growth and activities of sulphate-reducing bacteria in gut contents of healthy subjects and patients with ulcerative colitis. *FEMS Microbiology Ecology* 1991, 9(2):103-111.
51. Rey FE, Gonzalez MD, Cheng J, Wu M, Ahern PP, Gordon JI: Metabolic niche of a prominent sulfate-reducing human gut bacterium. *Proc Natl Acad Sci U S A* 2013, 110(33):13582-13587.
52. Shang Q, Sun W, Shan X, Jiang H, Cai C, Hao J, Li G, Yu G: Carrageenan-induced colitis is associated with decreased population of anti-inflammatory bacterium, Akkermansia muciniphila, in the gut microbiota of C57BL/6J mice. *Toxicol Lett* 2017, 279:87-95.

53. Li M, Li G, Zhu L, Yin Y, Zhao X, Xiang C, Yu G, Wang X: Isolation and characterization of an agaro-oligosaccharide (AO)-hydrolyzing bacterium from the gut microflora of Chinese individuals. *PLoS One* 2014, 9(3):e91106.
54. Bazzoni G: The JAM family of junctional adhesion molecules. *Curr Opin Cell Biol* 2003, 15(5):525-530.
55. Hajjari M, Behmanesh M, Sadeghizadeh M, Zeinoddini M: Junctional adhesion molecules 2 and 3 may potentially be involved in progression of gastric adenocarcinoma tumors. *Med Oncol* 2013, 30(1):380.
56. Lei F, Yin Y, Wang Y, Deng B, Yu HD, Li L, Xiang C, Wang S, Zhu B, Wang X: Higher-level production of volatile fatty acids in vitro by chicken gut microbiotas than by human gut microbiotas as determined by functional analyses. *Applied and environmental microbiology* 2012, 78(16):5763-5772.
57. Yin Y, Lei F, Zhu L, Li S, Wu Z, Zhang R, Gao GF, Zhu B, Wang X: Exposure of different bacterial inocula to newborn chicken affects gut microbiota development and ileum gene expression. *ISME J* 2010, 4(3):367-376.
58. Frank JA, Reich CI, Sharma S, Weisbaum JS, Wilson BA, Olsen GJ: Critical evaluation of two primers commonly used for amplification of bacterial 16S rRNA genes. *Appl Environ Microbiol* 2008, 74(8):2461-2470.
59. Tang QY, Zhang CX: Data Processing System (DPS) software with experimental design, statistical analysis and data mining developed for use in entomological research. *Insect Sci* 2013, 20(2):254-260.

Figures

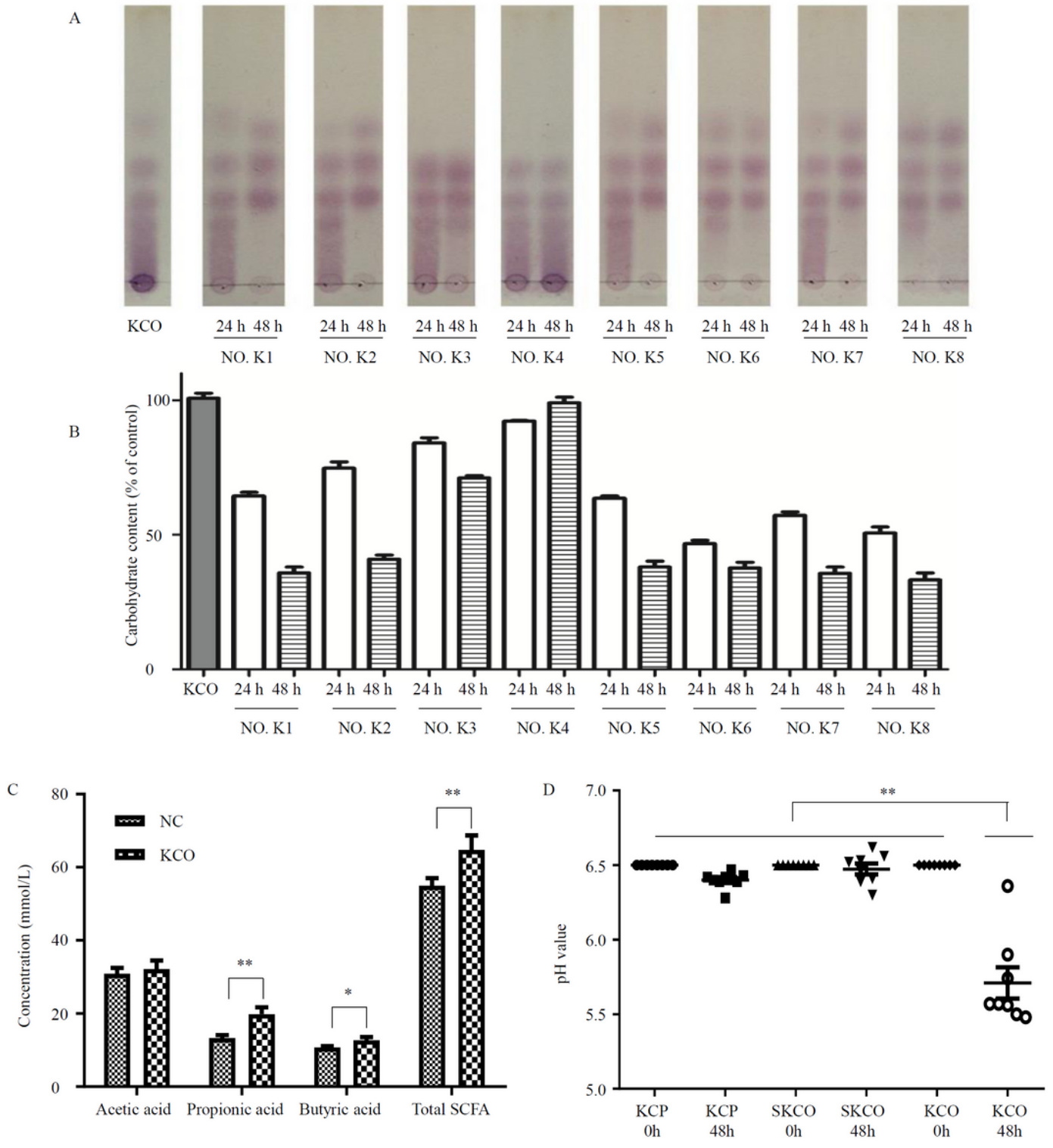

Figure 1

The degradation of KCOs by human fecal microbiota. A. The degradation of KCOs as measured by TLC. B. The average degradation rate of KCOs as measured using the phenol–sulfuric acid method. The degradation of KCOs by human gut microbiota was evaluated by TLC after fermentation in medium containing 8 g/L KCO for 24 and 48 hours. Control (KCO) is the medium without inoculation. Nos. 1–8 are fecal microbiota samples collected from healthy volunteers that were inoculated in the batch

chemostat. C. The effects of KCOs on SCFA production after 48 h of fermentation. Acetic, propionic, and butyric acid were detected by HPLC; total SCFA is the sum of acetic, propionic, and butyric acid. NC means no KCO was added (negative control). D. pH values before (0 h) and after (48 h) KCP, SKCO, and KCO fermentation. KCP, SKCO, and KCO represent CNGs with different MWs (KCP: 450 kDa; SKCO: 100 kDa; KCO: 4.5 kDa). *P < 0.05, **P < 0.001.

A

B

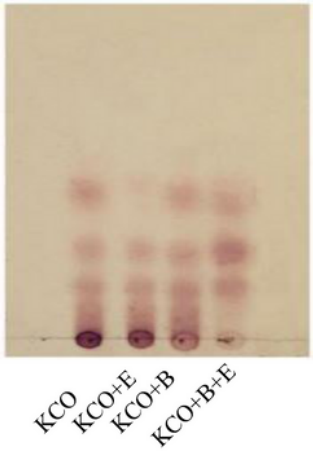

C

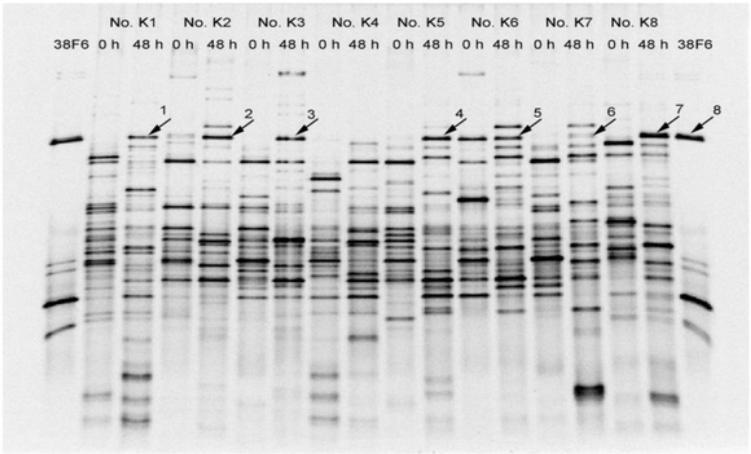

D

Band No.	Sample No.	Degradation Rates to KCO	Closed species	Similarity (%)
1	K1	63.7	*B. xylanisolvens*	100
2	K2	58.8	*B. xylanisolvens*	100
3	K3	29.1	Uncultured Firmicutes bacterium	100
-	K4	1.4	ND	ND
4	K5	61.5	*B. xylanisolvens*	100
5	K6	62.2	*B.xylanisolvens*	100
6	K7	63.7	Uncultured *Dialister sp.*	99
7	K8	65.8	*B. xylanisolvens*	100
8	Bx38F6	-	*B. xylanisolvens*	-

Figure 2

Identification of KCO degrading bacteria. A. Isolation and identification of the KCO degrading bacterium B. xylanisolvens. The KCO degradation ability of B. xylanisolvens isolate 38F6 as evaluated by TLC after fermentation in medium containing 8 g/l KCO for 48, 96, 144, and 192 hours. B. TLC analysis of KCO degradation by B. xylanisolvens and E. coli. Combination of B. xylanisolvens and E. coli synergistically increases KCO degradation. C. PCR-DGGE analysis of the bacterial community before (0 h) and after (48 h) KCO fermentation. Nos. K1–8 represent fecal microbiota samples collected from healthy volunteers that were inoculated in medium containing KCO (8 g/l) as the sole carbon source. Lane 38F6 represents PCR products that were obtained using B. xylanisolvens genomic DNA as template. Bands 1–8 correspond to the sequenced PCR-DGGE bands. D. Identification of bacterial species from PCR-DGGE bands 1–8 by BLAST alignment.

Figure 3

Structural changes in mouse intestinal sections after treatment with KCO and KCO degrading bacteria. Four groups of germ-free mice were included in the experiment, which lasted for 6 weeks. GFK and GNK groups were exposed to KCO (5% in drinking water) for the entire experiment. Mice in the GNK group were inoculated by oral gavage with B. xylanisolvens and E. coli (5×108) on day 0. The GN group was only inoculated with B. xylanisolvens and E. coli (5×108) on day 0. The GF group was the control group. A. Photomicrographs of representative HE staining in colon and rectum. B. Histopathological scores representing the severity of inflammation were taken in duodenum, jejunum, ileum, cecum, colon, and rectum. Results are expressed as mean ± SEM (n = 6). *P < 0.05, **P < 0.01.

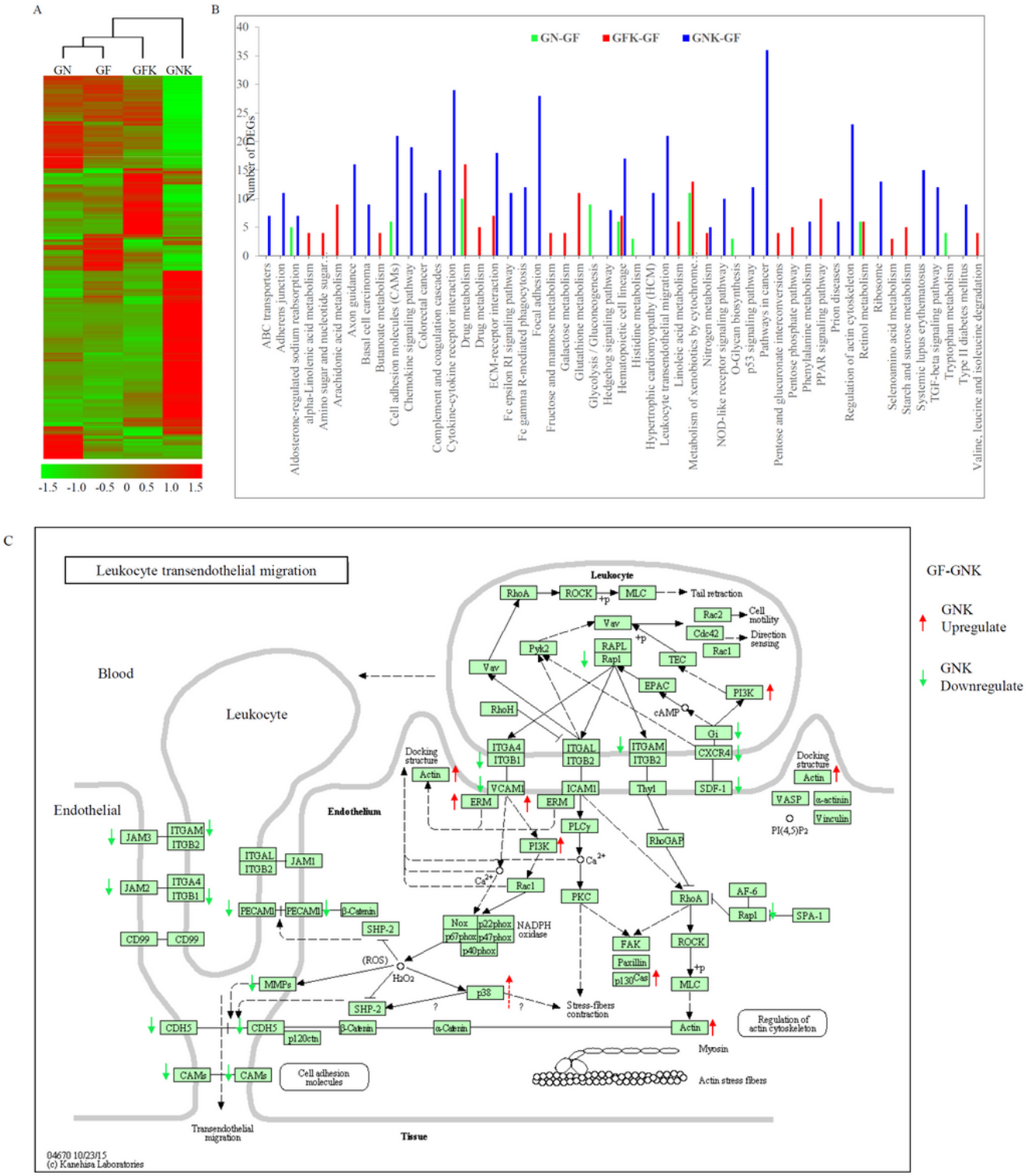

Figure 4

Comparison of DEGs in rectum tissue between different treatment groups. Germ-free mice were treated with KCO (5% in drinking water, GFK group), KCO plus B. xylanisolvens and E. coli (5×108, GNK group), only B. xylanisolvens and E. coli (5×108, GN group), or distilled water (GF, control group). Rectum samples were collected for RNA-Seq analysis. A. Heatmap depicting hierarchical clustering of the gene expression of rectum samples from different groups. Red and green represent up- and down-regulated expression,

respectively. Color density indicates the fold change. B. Number of genes taking part in the significantly differentially expressed KEGG pathways. C. Distribution of the DEGs on pathway Leukocyte transendothelial migration.

Figure 5

Immunohistochemical staining analysis of rectum samples. Four groups of germ-free mice were included in the experiment, which lasted for 4 months. Mice were treated with KCO (5% in drinking water, GFK group), KCO plus B. xylanisolvens and E. coli (5×108, GNK group), only B. xylanisolvens and E. coli (5×108, GN group), or distilled water (GF, control group). A. Photomicrographs of IHC staining against P-P38, CD3, CD79a, VCAM1 and PECAM1 in rectum tissue samples. B. Histopathological scores representing the severity of inflammation in rectum, after IHC staining results. Results are expressed as mean ± SEM (n = 6).

Supplementary Files

This is a list of supplementary files associated with this preprint. Click to download.

- KCOSupplementary20200501.pdf